Kind of Dual-band Horn Antenna with Coaxial Feed Structure for High Power Microwave Applications

Qiang Zhang, Sheng-Ren Peng, Cheng-Wei Yuan, Yi-Ming Yang, and Jing Liu
College of Optoelectronic Science and Engineering
National University of Defense Technology, Changsha 410073, China

Abstract— A new kind of dual-band horn antenna for S/X band radiation with high power handling capacity is proposed, which consists of coaxial feed structure flare angle horn and a polyethylene cover. Low band microwave is fed by TE_{11} coaxial waveguide mode, and high band microwave is fed by TE_{11} circular waveguide mode. Based on the specific structure of the horn antenna, mode matching method is utilized to determine scatter matrix of each discontinuity in cross section. To obtain the overall scatter matrix of the antenna, it is necessary to progressively cascade the scatter matrixes, and the overall scatter matrix determines the propagation properties of the horn antenna. Far field radiation pattern of the dual-band antenna can easily get by using mode expansion technology. Furthermore, a dual-band antenna at 3.6 GHz and 9.5 GHz is designed, and theoretical and numerical simulations agree well with each other. It reveals that the dual-band antenna has high power handling capacity with GWs level, and good farfield radiation pattern at each band has been achieved. The theoretical and numerical simulation investigations show that it is a promising method for realizing multi-channel multi-band HPM integrative radiation, which is significant for HPM in some special applications.

1. INTRODUCTION

With the development of high power microwave (HPM) technologies, great efforts have been made on increasing the output power levels and the frequency spectrum of the HPM systems [1]. An interesting direction for HPM development is to investigate devices capable of producing HPM with two stable and separate frequencies [2]. Therefore, extremely dual-band radiation systems [3] with high power-handling capacity are often required for many current applications. As one of the most important sectors in the HPM system, radiation system mainly determines the whole structure of the HPM system. On the other hand, narrow-band HPM source usually operates at single band and has limited output power at present. An alternative method for enhancing the output capacity of HPM system is taking advantage of waveguide-based power combining technologies, not only for increasing the output power levels, but also for the frequency spectrum of the HPM systems [4].

In this paper, a corrugated horn antenna for S/X band with special input port consisting of coaxial feed structure and a small flare angle horn is designed, and this antenna is utilized to radiate HPM in good far-field radiation at each band with high power handing capacity. The optimization has been achieved by mode matching method, and the results are confirmed by numerical simulations.

2. STRUCTURE OF THE ANTENNA

In order to radiate microwaves at each band with high power handing capacity, the designed antenna is shown in Fig. 1. The whole structure of the antenna is divided into three parts: First, the input port consists of a coaxial waveguide working at S-band and a small flare angle horn working at X-band, which realizes that microwaves at each band input through different feeding structure. Second, a circular waveguide with vertical corrugations plays an important part in the dual-band feed, insuring that E-plane and H-plane patterns of the antenna are almost equal to each other in the illuminated area at each band. Third, a plano-convex polyethylene lens cover is utilized to air proof the large flare angle horn, which increases the gain of the antenna to some extent, then the antenna can be pumped into high vacuum state and the electric breakdown threshold is higher than the one in atmosphere [1]. In some special application, this antenna can works as the feed of the near-field Cassegrain antenna.

3. ANALYSIS OF THE ANTENNA

In consideration of the azimuthally symmetric structure of the antenna, it can be regarded as consisting of a battery of discontinuities in cross section and short lengths of waveguides in isolation. Mode matching theory is an effective approach to obtain the overall scatter matrix from which

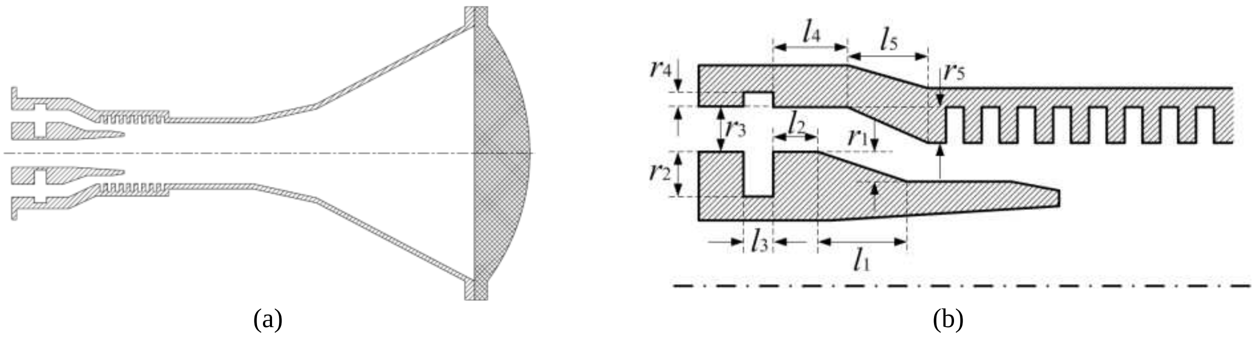

Figure 1: (a) Structure of the antenna. (b) Cross section of the coaxial feeding structure.

to determine the propagation properties of the antenna, which is extensively utilized to design overmoded mode converter and horn antenna [5, 6].

Concretely, we employ mode matching theory to get the scatter matrix of each discontinuity, which is progressively cascaded to obtain the overall scatter matric of the antenna. Using mode expansion technology in the aperture of the antenna, we can get the far-field radiation pattern of the horn antenna at last [7]. In general, the typical components of the antenna shown in Fig. 1 can be listed as follows in Fig. 2. The detail analysis process will be presented in another paper.

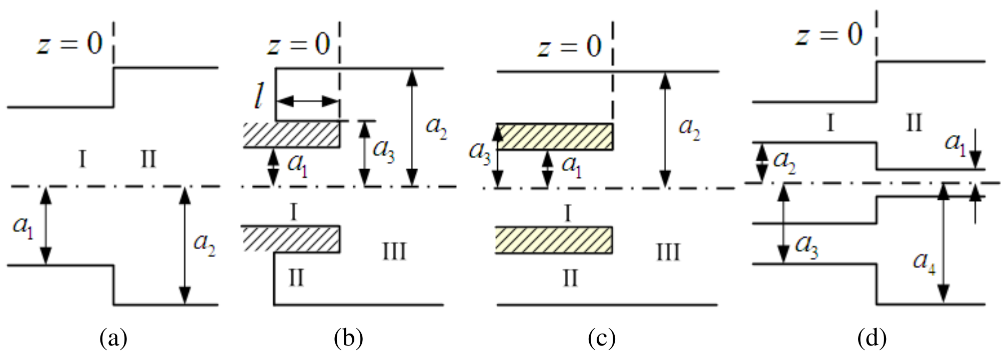

Figure 2: Typical components of the antenna.

Base on the propagation properties of the whole antenna, mode expansion technology is usually utilized to get the far-field radiation pattern of the antenna, by which we could analyse the contribution of each mode generated at the discontinuities makes to the far-field radiation pattern. In order to avoid radio-frequency (RF) electric breakdown occurring in atmosphere side near the outside of the cover, the aperture of the horn should be large enough to own high power handing capacity. We can not only employ aperture field theory to get the far-field radiation pattern of each mode at the aperture of the horn, but also decrease the calculation error generated by ignoring the surface current on the outside of the horn on the calculated far-field radiation pattern [7].

The radiation pattern of the antenna obtained by mode expansion technology can be written as

$$\begin{aligned} F(\theta,\phi) = & -\frac{C_{TE_{nm}} j^n kan}{\sqrt{\pi(u_{nm}^{*2}-n^2)}}\sqrt{\frac{\omega\mu}{\beta_{nm}^*}}\frac{e^{-jkR}}{R}\cos n\phi[1+t\eta\cos\theta+\Gamma(1-t\eta\cos\theta)]\frac{J_n(ka\sin\theta)}{ka\sin\theta} \\ & +\frac{C_{TE_{nm}} j^n ka}{\sqrt{\pi(u_{nm}^{*2}-n^2)}}\sqrt{\frac{\omega\mu}{\beta_{nm}^*}}\frac{e^{-jkR}}{R}\sin n\phi[\cos\theta+t\eta+\Gamma(\cos\theta-t\eta)]\frac{J_n'(ka\sin\theta)}{1-(\frac{ka\sin\theta}{u_{nm}^*})^2} \\ & -\frac{C_{TM_{nm}} j^n ka}{\sqrt{\pi}[(\frac{\chi_{nm}a}{ka\sin\theta})^2-1]}\sqrt{\frac{\beta_{nm}}{\omega\varepsilon}}\frac{e^{-jkR}}{R}\cos n\phi[(1+t\eta\cos\theta)+\Gamma(1-t\eta\cos\theta)]\frac{J_n(ka\sin\theta)}{ka\sin\theta} \end{aligned} \quad (1)$$

where, $u_{nm} = \chi_{nm}a$, $J_n(u_{nm}) = 0$, $u_{nm}^* = \chi_{nm}^* a$, $J_n'(u_{nm}^*) = 0$, a is the aperture radius, β_{nm} and β_{nm}^* denote propagation constant of TE_{1m} mode and TM_{1n} mode at the aperture, C_{TEnm} and C_{TMnm} denote complex coefficients of TE_{1m} mode and TM_{1n} mode respectively. By employing Eq. (1), one can obtain E-plane and H-plane radiation pattern under the condition of $\varphi = 0^\circ$ and $\varphi = 90^\circ$, respectively.

4. DESIGN AND NUMERICAL INVESTIGATION OF THE ANTENNA

4.1. Design of the Feeding Port with a Vertical Corrugations Structure

As shown in Fig. 3, the lens-horn antenna is fed by a coaxial waveguide working at S-band and an inner circular waveguide working at X-band, which is the basic component of the antenna. This structure provides the design possibilities to obtain good radiation characteristics at each band with a reasonable size capable of high power handing. The coaxial and circular waveguides are excited by the dominant TE_{11} mode and connected to the corrugated section. Considering its special structure, TE_{1n} and TM_{1n} modes can be excited at each discontinuity in the feed. Employing the optimization tools of CST software, dozens of different geometries have been analysed to reach the final design for the 3.60 and 9.50 GHz central frequency, with the dimensions as follows, $r_1 = 13.63$ mm, $r_2 = 22.59$ mm, $r_3 = 20$ mm, $r_4 = 9.44$ mm, $r_5 = 20.13$ mm, $l_1 = 38.28$ mm, $l_2 = 25.13$ mm, $l_3 = 19.31$ mm, $l_4 = 35.35$ mm, $l_5 = 43.06$ mm, and simulated results given in Fig. 4 to Fig. 5. The reflection of feeding port is quite small around the central frequency at each band, indicating the good transmission property of the feed. When the feeding port is fed with 1.0 W microwave, the maximum electric field strength is less than 702 V/m and 852 V/m, respectively. Generally, the feeding port is pumped into high vacuum state for HPM applications, in which the RF electric field breakdown threshold is greater than 1.0 MV/cm [9, 10]. Assuming the RF electric breakdown strength is 700 kV/cm, which has been confirmed in our recently HPM experiments [11], we can infer the maximum allowed input power for this feeding port is about 9.9 GW and 6.7 GW at S-band, X-band, respectively.

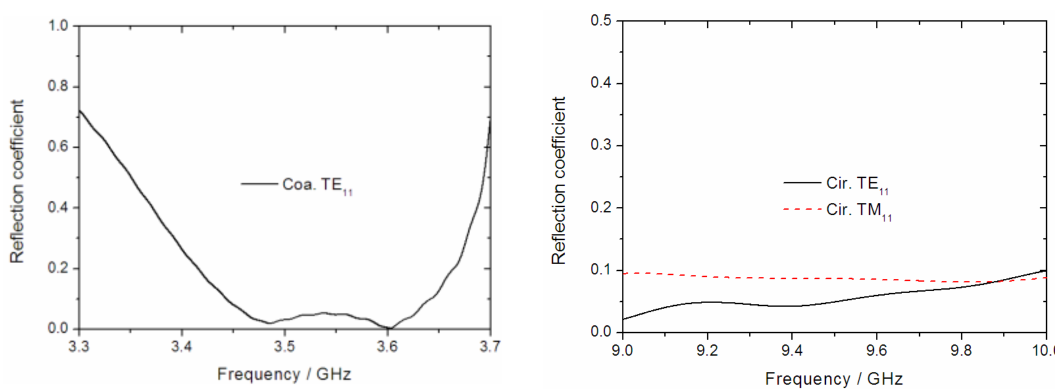

(a) S-band (3.60 GHz) (b) X-band (9.50 GHz)

Figure 3: Reflection coefficients versus frequency at each band.

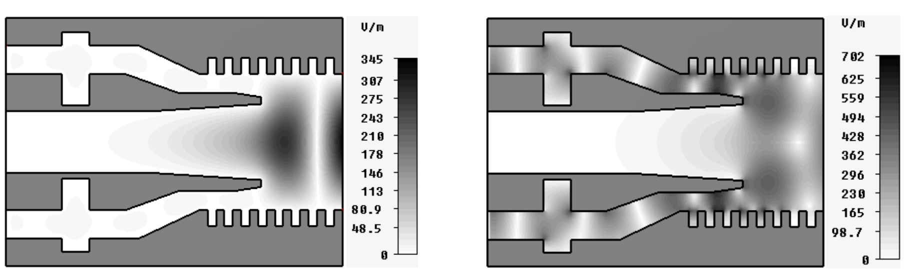

(a) S-band (3.60 GHz, *E*-plane) (b) X-band (9.50 GHz, *E*-plane)

Figure 4: Electric field distribution at each band.

4.2. Design of the Flare Angle Dielectric Lens-horn Antenna

The structure of flare angle antenna is optimized mainly by mode matching technology. In Section 4.1, the feeding port has reached the goal of good transmission property in dual-band, the remained works focus on the optimizing of the radiation property by elaborate design of the circular waveguide with vertical corrugations connected to the flare angle horn antenna. Fig. 6 shows the far-field radiation patterns of the horn antenna without dielectric cover, the theoretical results are

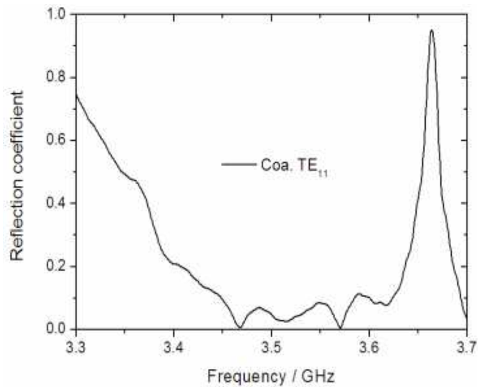

(a) S-band (3.60 GHz)

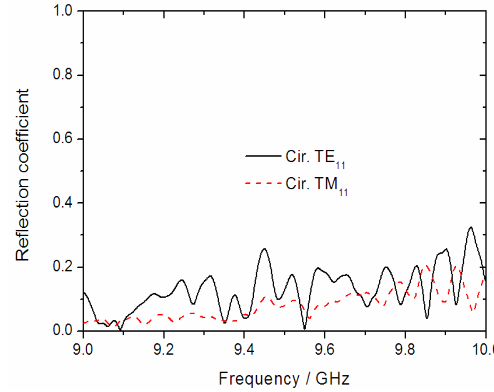

(b) X-band (9.50 GHz)

Figure 5: Reflection coefficients of the antenna at each band.

almost equal to the simulated noes. There is a little difference between the two results mainly for the reason that the surface current on the outside of the horn antenna is neglected in the calculation of the radiation pattern. From the simulated results, we can draw a conclusion that microwaves in dual-band are successfully radiated from the horn antenna, and the radiation patterns have the good performance of azimuthal symmetry, low side lobes, which lays the foundation of adding the dielectric lens cover to airproof the horn antenna.

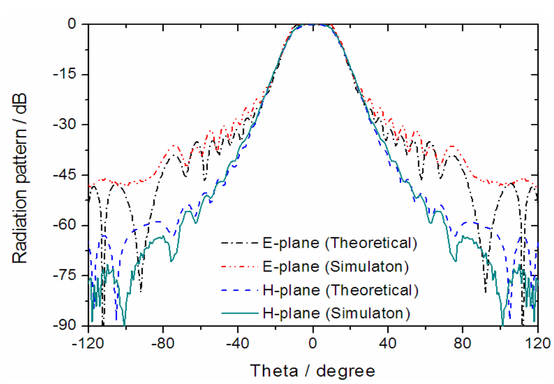

(a) S-band (3.60 GHz)

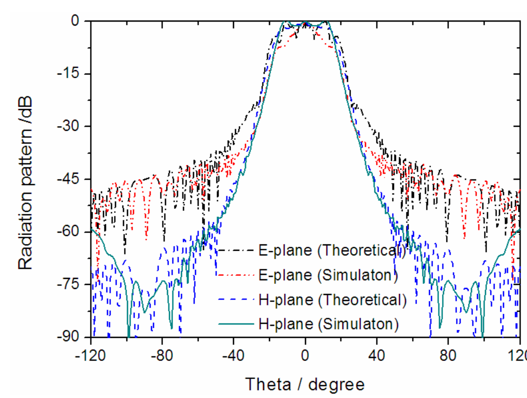

(b) X-band (9.50 GHz)

Figure 6: Radiation patterns of horn antenna without cover.

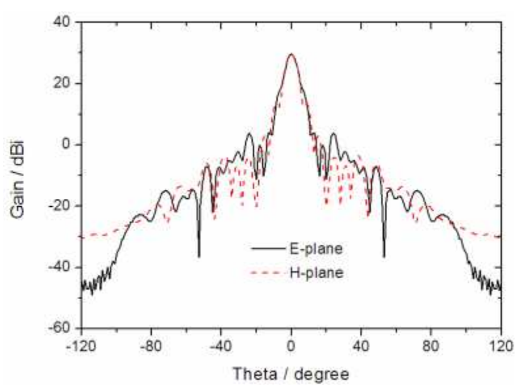

(a) S-band (3.60 GHz)

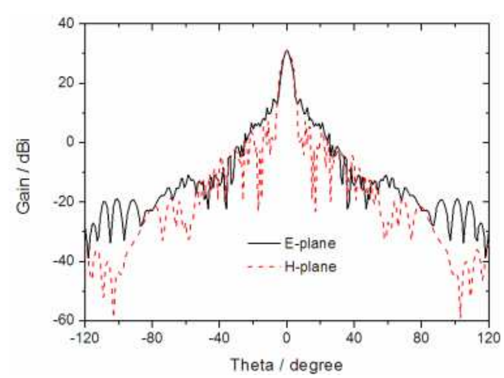

(b) X-band (9.50 GHz)

Figure 7: Far-field radiation pattern of the antenna at each band.

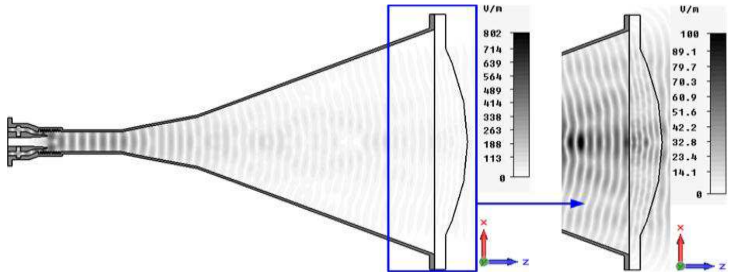

(a) S-band (3.60 GHz), E-plane

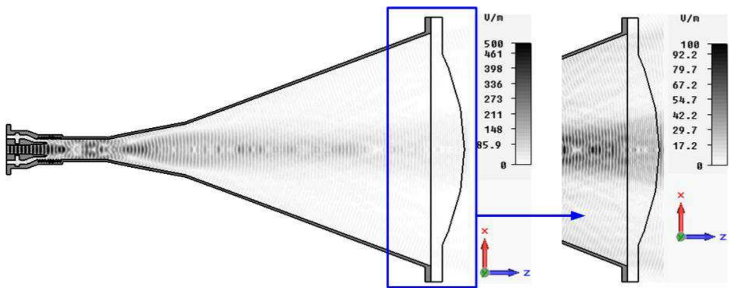

(b) X-band (9.50 GHz), E-plane

Figure 8: Electric field distribution of the lens-horn antenna.

Dielectric lens is widely used in the design of the antenna in the traditional communication field [12–14]. On the one hand, the horn antenna covered by dielectric lens can be pump into high vacuum state, and the RF breakdown threshold in the horn antenna is higher than the one in atmosphere. On the other hand, the quasi sphere wave in the horn is transformed to plane wave when it gets through the cover, which enhancing the gain of the horn antenna. Yuan has done plenty investigations about lens cover for high power microwave application and obtained a lot of valuable results [15]. A wide bandwidth plano-convex dielectric lens cover is investigated to airproof the dual-band horn antenna designed above.

To verify the feasibility of the whole antenna, the dual-band dielectric lens-horn antenna connected feeding port is simulated by the numbers. A small reflection caused by the cover has little influence on the good propagation property of the horn antenna. Fig. 7 presents the favourable radiation patterns of the lens-horn antenna. It is obvious that E-plane and H-plane patterns of the antenna are almost equal to each other in the illuminated area.

The electric field distributions in the horn and outside the cover are shown in the Fig. 8. The quasi sphere wave propagate in the horn, then transformed to plane wave by the cover, which makes the field distribution almost uniform in the aperture of the antenna. The maximum electric field lies in the feeding port, which limits the power handing capacity of the whole antenna. In the practical application, we can optimize the structure of the feeding port to increase the power handing capacity if it is needed.

According to the simulation, the input power is 1.0 Watt, the electric field distribution of the antenna is shown in Fig. 8. Outside the lens cover, the electric field strength is less than 0.43 V/cm at 3.60 GHz and 0.65 V/cm at 9.50 GHz, respectively. Assume the breakdown threshold in atmosphere under the condition of short microwave duration is about 3×10^4 V/cm, so the power breakdown threshold in this area is about $(3 \times 10^4/0.65)2 = 2.3$ GW. As the maximum allowed input power mentioned above for this feeding port is about 9.9 GW and 6.7 GW at S-band, X-band, respectively it means that the electric breakdown will take place in the near field outside the cover of the antenna. As a result, we estimate that the power-handling capacity of the dual-band horn antenna is about 2.3 GW.

5. CONCLUSION

This paper has presented a general study of the dual-band horn antenna with coaxial feed structure. The antenna's far-field radiation patterns belonging to each band have been confirmed by simulation. In addition, the radiation system is large enough for high power handling capacity, and experimental research is planned for the next step in order to make sure the sufficient power handling capacity.

REFERENCES

1. Benford, J., J. A. Swegle, and E. Schamiloglu, *High Power Microwaves*, 2nd Edition, Taylor & Francis, New York, 2007.
2. Fan, Y. W., et al., "A double-band high-power microwave source," *J. Appl. Phys.*, Vol. 102, No. 10, 303–304, 2007.
3. Imbriale, W. A., "An alternative feed design for the MRO antenna," *Proc. IEEE Antennas Propag. Soc. Int. Symp.*, Vol. 3A, 761–764, 2005.
4. Zhang, Q., C. W. Yuan, and L. Liu, "Design of a dual-band power combining architecture for high-power microwave applications," *Laser and Particle Beams*, Vol. 28, 377–385, 2010.
5. James, G. L., "Analysis and design of TE_{11}-to-HE_{11} corrugated cylindrical waveguide mode converters," *IEEE Trans. Microw. Theory and Techni.*, Vol. 29, No. 10, 1059–1066, 1981.
6. James, G. L., "On the problem of applying mode-matching techniques in analyzing conical waveguide discontinuities," *IEEE Trans. Microw. Theory and Techni.*, Vol. 31, No. 9, 718–723, 1983.
7. Ren, L., *Theory Foundation of Antenna*, Posts & Telecom Press, Beijing, 1980.
8. Cooper, D. N., "Complex propagation coefficients and the step discontinuity in corrugated cylindrical waveguides," *Electron. Lett.*, Vol. 7, 135–136, 1971.
9. Robert, J. B. and S. Edl, *High-power Microwave Sources and Technologies*, IEEE Press, Piscataway, NJ, 2001.
10. Xiao, R. Z., C. H. Chen, W. Song, et al., "A high-power high-efficiency klystronlike relativistic backward wave oscillator with a dual-cavity extractor," *Appl. Phys. Lett.*, Vol. 98, No. 10, 101502, 2011.
11. Zhang, J., Z. X. Jin, J. H. Yang, et al., "Recent advance in long-pulse HPM sources with repetitive operation in S-, C-, and X-bands," *IEEE Trans. Plasma*, Vol. 39, No. 6, 1438–1445, 2011.
12. Rozenfeld, P., "The electromagnetic theory of three-dimensional inhomogeneous lenses," *IEEE Trans. Antennas Propag.*, 366–370, 1975.
13. Fernandes, C. A., "Shaped dielecyric lenses for wireless millimeter-wave communicatioins," *IEEE Trans. Antennas Propag.*, Vol. 41, No. 5, 356–365, 1999.
14. Min, S., H. Jung, G. Park, et al., "Mode conversion of high-power electro- magnetic microwave using coaxial-beam rotating antenna in relativistic backward-wave oscillator," *IEEE Trans. Plasma Sci.*, Vol. 38, No. 6, 1391–1397, 2010.
15. Yuan, C. W., "Investigations of novel coaxial mode converters and mode-transducing antennas for high-power microwave," National University of Defense Technology, 2006.